# Impurity incorporation and doping efficiency in *a*-Si:H

K. Winer,* R. A. Street, N. M. Johnson, and J. Walker
*Xerox Corporation, Palo Alto Research Center, Palo Alto, California 94304*
(Received 26 January 1990)

A chemical equilibrium model of impurity incorporation in *a*-Si:H leads to a simple expression for the doping efficiency $\eta$ of substitutional impurities $I$ in terms of the impurity distribution coefficient, $d(I)$, and the gas-phase impurity mole fraction, $X_I$; $\eta \equiv [I_4]/[I] \propto (d(I))^{-1} X_I^{-1/2}$. In order to test this model, the distribution coefficients of As and P were measured over a wide range of *a*-Si:H deposition conditions from which $\eta$ and the impurity incorporation rate were determined. An approximate analytical expression for $d(I)$ has been fitted to the data and various impurity-incorporation mechanisms are considered to account for its form. The resulting intuitive, analytical expressions for the incorporation rate and doping efficiency of substitutional impurities in *a*-Si:H are valid for most deposition conditions.

## I. INTRODUCTION

Impurity incorporation in hydrogenated amorphous silicon (*a*-Si:H) has been an active area of research ever since substitutional doping was first discovered in this material by Spear and LeComber in 1975.[1] Early attention was directed toward measuring the doping efficiency $\eta$, defined as the fraction of electronically active impurity atoms incorporated during *a*-Si:H growth.[2] The efficiency is less than unity because impurities can be incorporated into either threefold- or fourfold-coordinated sites, and only the latter are electronically active. The doping efficiency also depends on the impurity incorporation probability from the deposition plasma. This probability is defined in terms of the distribution coefficient $d$, which is the ratio of the solid- and gas-phase impurity mole fractions,

$$d(I) \equiv \frac{[I]}{[\mathrm{Si}]} \frac{1}{X_I} . \quad (1)$$

$I$ represents the impurities, the brackets represent solid-phase concentrations, and $X_I$ is the gas-phase impurity mole fraction (e.g., for phosphorus $X_\mathrm{p} \equiv [PH_3]/\{[SiH_4]+[PH_3]\}$). The different coordination states of the atoms are represented in the following by subscripts enclosed in parentheses (e.g., $I_{(4)}$, $\mathrm{Si}_{(3)}$, etc.), and the absence of a subscript implies the total concentration.

The doping efficiency can be expressed in terms of either the gas- or solid-phase impurity mole fractions as follows:[3]

$$\eta_\mathrm{solid} \equiv \frac{[I_{(4)}]/[\mathrm{Si}]}{[I]/[\mathrm{Si}]} = \frac{1}{d(I)} \frac{[I_{(4)}]/[\mathrm{Si}]}{X_I} \equiv \frac{1}{d(I)} \eta_\mathrm{gas} . \quad (2)$$

$\eta_\mathrm{solid}$ and $\eta_\mathrm{gas}$ are equal when $d(I)$ is unity. Measurements of the boron and phosphorus distribution coefficients typically find values up to 30 at low $X$, which decrease to $\approx 3$ at high $X$.[4] However, the arsenic distribution coefficient is much larger, with values up to 300, and displays a stronger dependence on $X$. One might expect the solid-phase doping efficiency $\eta_\mathrm{solid}$ to be constant and the gas-phase doping efficiency $\eta_\mathrm{gas} \propto d(I)$ to depend strongly on the impurity. The puzzling result is that exactly the opposite occurs. $\eta_\mathrm{gas}$ is the same for phosphorus and arsenic, while $\eta_\mathrm{solid}$ is quite different, even though both are group-V substitutional dopants.[3] The key to understanding this result lies in the detailed behavior of the distribution coefficient as a function of the growth conditions.[4]

Deposition of *a*-Si:H films is primarily from radicals created by the plasma, and the dissociation rate depends on the molecular species. The concentration of silane and impurity-containing radicals is proportional to the gas-phase mole fractions $X_\mathrm{Si}$ and $X_I$, respectively. The resulting impurity distribution coefficient $d(I)$ is determined by the relative rates of silane and impurity gas dissociation and, in general, is different from unity. According to Henry's law, $d(I)$ should be independent of the gas composition at low $X_I$. Actually, $d(I)$ varies strongly with composition, particularly for arsenic doping. The only explanation of the strong dependence of $d(I)$ on $X_I$ is that there are complex chemical reactions occurring during growth which are not described by the simple power-dependent creation of gas radicals and which involve large mole fractions of As-containing species. A general thermodynamic analysis of *a*-Si:H growth allows the general properties of these reactions to be obtained from impurity incorporation and doping efficiency measurements.

## II. MODEL OF EQUILIBRIUM *a*-Si:H GROWTH

The model assumes that the growth of *a*-Si:H occurs close to equilibrium. The assumption is obviously questionable, since (a) the amorphous phase is not the thermodynamic ground state of silicon and (b) the plasma is not an equilibrium gas. However, the following justifications can be offered.

(1) The plasma creates radicals which chemically react

 

with the surface, but apparently does not play any further role in the deposition. The assumption that these radicals can achieve a chemical equilibrium with the a-Si:H growth surface under certain deposition conditions is plausible.

(2) Many aspects of a-Si:H deposition are characteristic of quasiequilibrium growth.[5] At low plasma power the deposition is close to chemical-vapor-deposition conditions, described by a low sticking coefficient and with a growth rate which is not limited by the flux of radicals from the gas.

(3) Of all the deposited species considered here, the large concentration of fourfold-coordinated silicon is the least likely to be in equilibrium. However, our model primarily focuses on impurity and defect species present in much lower concentrations. The chemical reactions that control dopant activation and defect formation are known to reach equilibrium at the deposition temperature, where atomic hydrogen can diffuse freely in and out of the growing surface and promote equilibration.[6] The nonequilibrium nature of the silicon network does not preclude equilibration between the minority species it hosts.

The model is an extension of the doping model which successfully accounts for the presence of defects in doped a-Si:H.[7] Substitutional dopants produce compensating charged defects which limit the extrinsic carrier concentration in a-Si:H. These defects are explained by a chemical equilibrium between threefold- and fourfold-coordinated silicon (Si) and impurities ($I$) according to the following reaction:

$$\mathrm{Si}_{(4)}+I_{(3)}\leftrightarrows I^{+}_{(4)}+\mathrm{Si}^{-}_{(3)} \ . \tag{3}$$

The application of this reaction to doped a-Si:H is discussed in more detail elsewhere.[7] Experiments have shown that the majority of dopants in a-Si:H are ionized, so that $[I^{+}_{(4)}]\simeq[I_{(4)}]$.[7] Also, the density of band tail electrons is usually less than 10% of $[I_{(4)}]$ and, therefore, can be neglected in the present analysis. With these approximations, application of the law of mass action to reaction (3) predicts a square-root dependence of the defect concentration $[\mathrm{Si}^{-}_{(3)}]$ and doping efficiency on the solid-phase impurity concentration:

$$[\mathrm{Si}^{-}_{(3)}]=[I^{+}_{(4)}]\propto[I]^{1/2}, \quad \eta_{\mathrm{solid}}\propto[I]^{-1/2} \ . \tag{4}$$

Measurements find that this relation is obeyed when $[I]$ is replaced with $X_I$ in Eq. (4), which is expected if the solid- and gas-phase mole fractions are proportional.[3] Furthermore, the expected temperature dependence of the equilibrium doping efficiency from reaction (3) is also observed.[6]

Reaction (3) only considers equilibration within the solid. It can be extended to include the growth process by considering the following four deposition reactions describing the incorporation of the four species of Si and $I$ in reaction (3):[4]

$$\mathrm{Si}^{G}\leftrightarrows\mathrm{Si}_{(4)}, \quad [\mathrm{Si}_{(4)}]=K_1X_{\mathrm{Si}}\simeq K_1 \ ; \tag{5}$$

$$\mathrm{Si}^{G}\leftrightarrows\mathrm{Si}^{-}_{(3)}-e^{-}, \quad [\mathrm{Si}^{-}_{(3)}]/[e^{-}]=K_2X_{\mathrm{Si}}\simeq K_2 \ ; \tag{6}$$

$$I^{G}\leftrightarrows I_{(3)}, \quad [I_{(3)}]=K_3X_I \ ; \tag{7}$$

$$I^{G}\leftrightarrows I^{+}_{(4)}+e^{-}, \quad [e^{-}][I^{+}_{(4)}]-K_4X_I \ . \tag{8}$$

The equations on the right are mass-action solutions to the reactions, with reaction constants $K_1$, $K_2$, $K_3$, and $K_4$. $X_a$ is the gas-phase mole fraction and $[a]$ is the solid-phase concentration of species $a$. The formation of charged coordination defects $\mathrm{Si}^{-}_{(3)}$ and active donors $I^{+}_{(4)}$ is described by the extra electron in Eqs. (6) and (8). Throughout our analysis it is assumed that the incorporation rates of the different species (as described below by rate constants $k_I$, $k_{\mathrm{Si}_{(3)}}$, etc.) are proportional to the reaction constants.

When the deposition is described precisely by any one of the above reactions, then each reaction constant $K$ is solely a function of temperature and is regular (i.e., independent of the gas-phase mole fraction of any species). However, if there are chemical processes which are not described by the reactions, then the observed values of $K$ will not be constant and will have irregular behavior. The purpose of the analysis is to determine which of the $K_i$ are irregular and, thereby, to identify which of the deposition processes cannot be described by the simple reactions (5)–(8). As an example, one might anticipate two channels of impurity incorporation in plasma-enhanced chemical vapor deposition (PECVD); a plasma-enhanced mode where the incorporation rate is independent of substrate temperature and a pyrolytic mode where the incorporation rate is independent of plasma power. Under very-low-power growth conditions, growth rates (i.e., PECVD incorporation rates) are low and thermally driven surface chemical reactions are more likely to dominate impurity incorporation than at high plasma powers. Such chemical reactivity during growth would be manifested by irregularities in the impurity incorporation rates, which would lead to the irregular behavior of one or more of the reaction constants $K_i$.

Equations (5)–(8) imply equilibration both at the surface and within the solid, and can be solved in terms of either the gas- or solid-phase concentrations. The concentration of band-tail electrons is small enough to be neglected (i.e., $[\mathrm{Si}^{-}_{(3)}]\simeq[I^{+}_{(4)}]$). Hence, in terms of the gas-phase concentrations,

$$[\mathrm{Si}^{-}_{(3)}]\simeq[I^{+}_{(4)}]=(K_2K_4X_{\mathrm{Si}}X_I)^{1/2} \simeq(K_2K_4X_I)^{1/2} \ , \tag{9}$$

and, in terms of the solid-phase concentrations,

$$[\mathrm{Si}^{-}_{(3)}]\simeq[I^{+}_{(4)}]=\left[\frac{K_2K_4}{K_1K_3}[\mathrm{Si}_{(4)}][I_{(3)}]\right]^{1/2} \simeq\left[\frac{K_2K_4}{d(I)}\frac{[I]}{[\mathrm{Si}]}\right]^{1/2} , \tag{10}$$

where the distribution coefficient has been written in terms of the reaction constants as follows:

$$d(I)=\frac{[I]}{[\mathrm{Si}]}\frac{1}{X_I}\simeq\frac{[I_{(3)}]}{[\mathrm{Si}_{(4)}]}\frac{1}{X_I}=\frac{K_3}{K_1} \ . \tag{11}$$

The approximations in Eqs. (9)–(11) are valid because

most of the substitutional impurity and Si atoms are threefold- and fourfold-coordinated, respectively.[7]

Equations (9) and (10) predict the following. The defect concentration $[Si_{(3)}^-]$ follows a square-root law with $X_I$ provided $K_2$ and $K_4$ are regular (i.e., independent of impurity concentration), which is expected for very dilute phases from Henry's law. However, $[Si_{(3)}^-]$ will follow a square-root law with $[I]$ *only* when $K_3$ [and, therefore, $d(I)$] is also regular. These predictions provide an immediate interpretation of the experimental evidence. The square-root dependence of $[Si_{(3)}^-]$ on $X_I$ is always observed and indicates that $K_2$ and $K_4$ are indeed regular. Thus the incorporation of active dopants is adequately described by reaction (8). The square-root dependence of $[Si_{(3)}^-]$ on the solid-phase impurity concentration $[I]$ is not always observed. However, deviations from this dependence are always accompanied by an irregular (i.e., concentration-dependent) distribution coefficient. This means that the incorporation of inactive impurities is governed by processes which are not adequately described by reaction (7).

The solid- and gas-phase doping efficiencies according to the equilibrium growth model under the assumption that $K_2$ and $K_4$ are regular become

$$\eta_{\text{solid}} \equiv \frac{[I_{(4)}]/[\text{Si}]}{[I]/[\text{Si}]} \propto \frac{1}{d(I)} X_I^{-1/2} ,$$
$$\eta_{\text{gas}} \equiv \frac{[I_{(4)}]/[\text{Si}]}{X_1} \propto X_I^{-1/2} . \tag{12}$$

The model predicts that $\eta_{\text{gas}}$ will depend on $X_I$ in the same way for all impurities, as observed, while $\eta_{\text{solid}}$ depends strongly on the behavior of the distribution coefficient. Thus $\eta_{\text{solid}}$ should also depend strongly on the conditions of growth, even though $[I_{(4)}^+]$ does not. This is because it is $K_3$ and the incorporation of $I_{(3)}$, not $I_{(4)}^+$, which displays irregular behavior.

The applicability of this chemical equilibrium model to $n$-type $a$-Si:H growth has been tested by measuring the defect concentrations and impurity distribution coefficients in P- and As-doped $a$-Si:H over a range of deposition conditions.[4] Here we extend this range, derive analytical expressions for the As distribution coefficient, As incorporation rate, and As doping efficiency valid for most deposition conditions, and explore additional chemical models to account for the functional form of $d(I)$ derived by fitting to the data.

## III. EXPERIMENTAL RESULTS

For the measurements, thin single- and multiple-layer films of either P- or As-doped $a$-Si:H were deposited onto glass substrates held at 230 °C by the rf glow-discharge decomposition of phosphine/silane or arsine/silane gas mixtures. The rf power was varied between 1 and 60 W, and the dopant gas ratios were varied between $3\times10^{-6}$ and $1\times10^{-3}$. The film growth rates were approximately proportional to the rf power and were essentially independent of the dopant gas concentration. The defect concentrations were determined from optical absorption spectra measured by photothermal deflection spectroscopy.[8] The impurity distribution coefficients were determined from the As and P concentrations measured by secondary-ion-mass spectrometry.[9] The determinations from both methods are accurate to within a factor of 2.

As distribution coefficients were also determined from samples prepared by the decomposition of silane/arsine gas mixtures in a remote hydrogen plasma reactor described elsewhere.[10] The film growth rates were proportional to the microwave plasma power and total gas flow, and were as much as 8 times lower than those of samples prepared under standard 2-W rf glow-discharge deposition conditions. The lower growth rates allow the irregular incorporation behavior of As to be studied over a correspondingly greater range.

### A. Defect concentrations

Figure 1 indicates that the defect concentrations in both P- and As-doped $a$-Si:H are essentially the same for a given value of $X$ and increase as the square root of $X$ even at high rf power. This result confirms the expected regularity of $K_2$ and $K_4$, and shows that the concept of the equilibrium interconversion of threefold- and fourfold-coordinated dopant configurations appears to be valid for both P- and As-doped $a$-Si:H. In addition, the absolute defect concentrations and dark dc conductivities (i.e., carrier concentrations) and their dependence on thermal history are virtually identical in P- and As-doped $a$-Si:H.[6] The bulk equilibration processes, therefore, involve approximately the same concentrations of interconverting threefold- and fourfold-coordinated dopants in both materials. However, the absolute concentrations of As and P under identical deposition conditions are not the same.

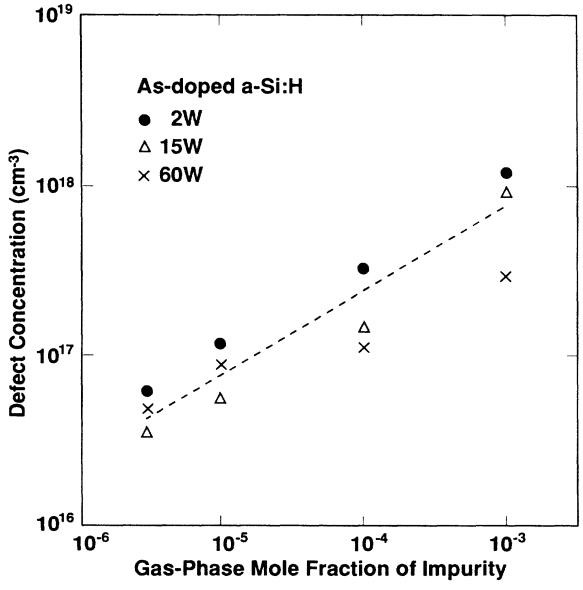


FIG. 1. Defect concentration as a function of mole fraction of impurity gas for As-doped $a$-Si:H deposited at 2 W (solid circles), 15 W (open triangles), and 60 W (crosses). Dashed line denotes dependence of P-doped $a$-Si:H deposited at 2 W from Ref. 3.

### B. Distribution coefficients

The As and P distribution coefficients of a-Si:H deposited by rf glow discharge are plotted in Figs. 2(a) and 2(b) over a range of rf power and $X$. The As distribution coefficient varies the most, with values ranging from 6 to 300. $d$(As) is as much as 10 times larger than $d$(P) under typical low-power deposition conditions and is always higher than $d$(P) at the same rf power and $X$. The As and P distribution coefficients are both highly irregular at low rf power. They can be described by two terms: a regular constant value $d_{reg}$, and an irregular term varying with rf power $E$ and gas-phase mole fraction $X$:

$$d = d_{reg} + d_{irreg}(E,X) \approx d_{reg} + \beta X^{-1/2}/(\alpha E) , \qquad (13)$$

where $\alpha E$, with $\alpha \simeq 0.25$ Å/W s, is defined as the film growth rate. Equation (13) is an approximate analytical expression for $d$ and has been fitted to the data with $d_{reg}=8$ and $\beta=0.13$ Å/s for As, and $d_{reg}=3$ and $\beta=0.009$ Å/s for P, as shown in Figs. 2(a) and 2(b).

The large distribution coefficient suggests the possibility of significant depletion of the arsine from the plasma. The total gas flow rate used in the reactor is 100 sccm. An arsine mole fraction of $10^{-6}$ corresponds to an incoming flow of $4.5\times10^{13}$ As molecules/s. The growth rate at 1 W rf plasma power is about 0.5 Å/s, which corresponds to a flux of $3\times10^{8}$ As atoms/(cm$^2$ s). The distribution coefficient under these conditions is $\approx 300$, and the area of deposition is $\approx 100$ cm$^2$, so that an estimated $(9.0\times10^{12})/(4.5\times10^{13})=20\%$ of the arsine gas is incorporated into the a-Si:H film under the most irregular growth conditions. Arsine depletion would be marked by a saturation in the distribution coefficient at a particular value. From the data so far available, this saturation limit must lie above $d \approx 1000$.

The As distribution coefficients for a-Si:H deposited by remote hydrogen plasma decomposition are plotted in Figs. 3(a) and 3(b) as a function of deposition rate and $X$ to facilitate comparison with the distribution coefficients of the glow-discharge films. a-Si:H produced under 50:25 $H_2$:$SiH_4$ dilution was grown at rates between 2 and 4 times lower than the lowest rf glow-discharge growth rates. The resulting As distribution coefficients are correspondingly larger, with the overall trend consistent with Eq. (13). This confirms that, except for the lower growth rates due to $H_2$ dilution, remote hydrogen plasma deposition is identical to rf glow-discharge deposition.[10] This further implies that the effects of the plasma such as ion bombardment and uv light exposure do not affect impurity incorporation in a-Si:H. The As distribution coefficient for a-Si:H grown under 200:100 $H_2$:$SiH_4$ dilution is anomolously larger, indicating that deposition parameters other than the growth rate and gas-phase impurity mole fraction can influence impurity incorporation.

It might be expected that subtle effects of the deposition parameters on impurity incorporation might become more apparent under low-growth-rate conditions, where the solid and gas phases are closer to chemical equilibrium. However, the dependence of $d$(As) on gas flow rate (Fig. 4) and substrate temperature (Fig. 5) are relatively

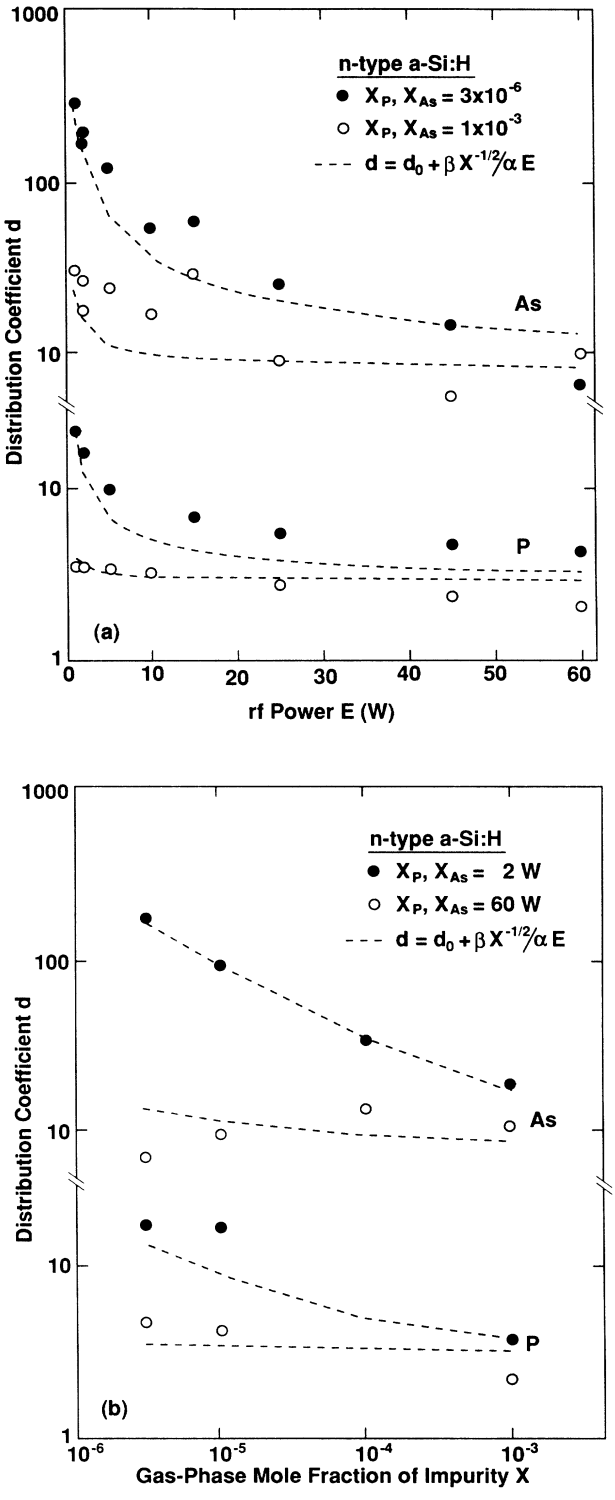


FIG. 2. (a) Distribution coefficients as a function of rf power for As- and P-doped a-Si:H for gas-phase impurity mole fractions of $3\times10^{-6}$ (solid circles) and $1\times10^{-3}$ (open circles). Dashed lines are the fits to the data using Eq. (13) with $d_{reg}=8$ and $\beta/\alpha=0.51$ W for As, and $d_0=3$ and $\beta/\alpha=0.035$ W for P. (b) Distribution coefficients as a function of mole fraction of impurity gas for As- and P-doped a-Si:H deposited by rf glow discharge at 2 W (solid circles) and 60 W (open circles). Dashed lines are the fits to the data using Eq. (13) with $d_{reg}=8$ and $\beta/\alpha=0.51$ W for As, and $d_0=3$ and $\beta/\alpha=0.035$ W for P.

weak; less than a factor of 2 for a factor of 4 change in flow rate or growth temperature. Also, the direction of change is not what might be expected. For example, if $d$(As) is dominated by a pyrolytic process at low growth rates, one would expect $d$(As) to increase, not decrease, with increasing substrate temperature. We return to this issue in the discussion.

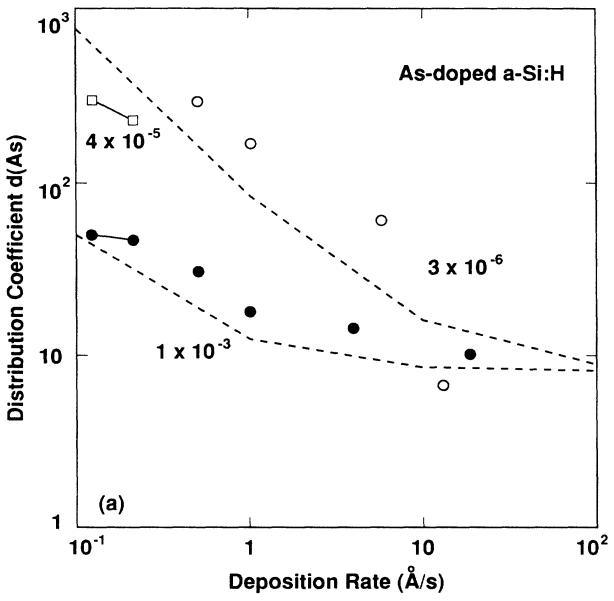


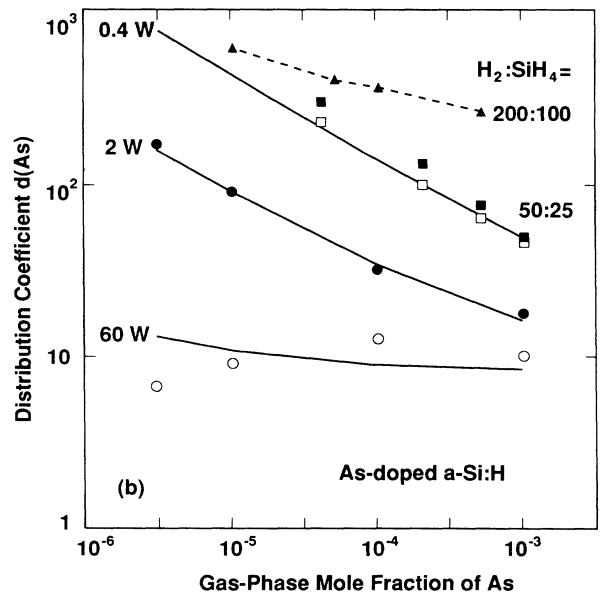


FIG. 3. (a) Distribution coefficients as a function of deposition rate for As-doped $a$-Si:H. The two pairs of data points at the lowest deposition rates were grown in a remote hydrogen plasma reactor under 50:25 $H_2$:$SiH_4$ dilution. Data from Fig. 2(a) are included for comparison. Dashed lines are calculated using Eq. (13) with $d_{reg}=8$ and $\beta/\alpha=0.51$ W. (b) Distribution coefficients as a function of mole fraction of impurity gas for As-doped $a$-Si:H deposited by rf glow discharge at 2 and 60 W, and by remote hydrogen plasma deposition at 50:25 $H_2$:$SiH_4$ dilution (75 and 150 W microwave power), and at 200:100 $H_2$:$SiH_4$ dilution (75 W). Curves are $d$(As) calculated using Eq. (13) with $d_{reg}=8$ and $\beta/\alpha=0.51$ W for 0.4, 2, and 60 W rf power.

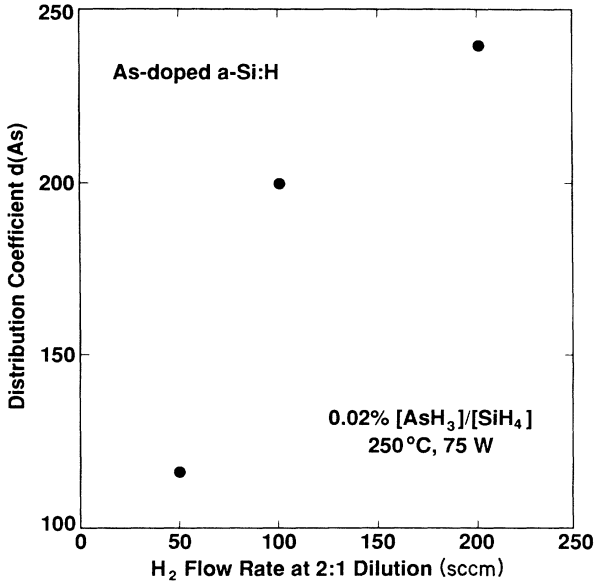


FIG. 4. Distribution coefficient as a function of $H_2$ gas flow rate under 2:1 $H_2$:$SiH_4$ dilution for As-doped $a$-Si:H deposited in a remote hydrogen plasma reactor [units are given in cubic centimeters per minute at STP (sccm)].

### C. As incorporation rate

Rewriting Eq. (13) as the ratio of As and Si incorporation rates $r$, we obtain

$$d(\mathrm{As})=r_{\mathrm{As}}/(r_{\mathrm{Si}}X_{\mathrm{As}})\ . \tag{14}$$

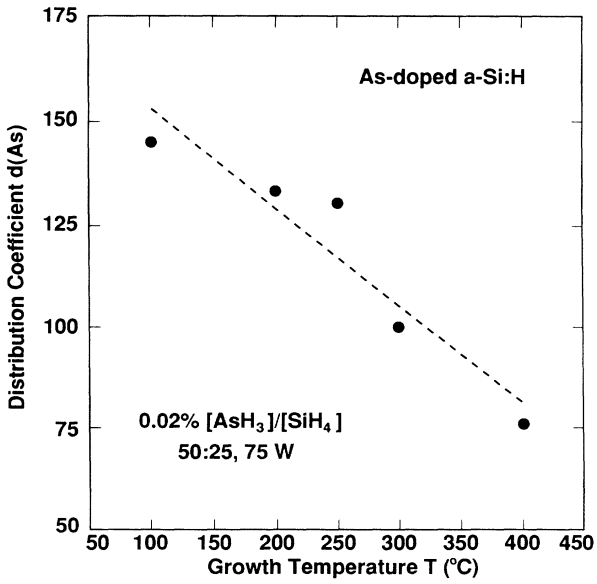


FIG. 5. Distribution coefficient as a function of growth temperature for As-doped $a$-Si:H deposited in a remote hydrogen plasma reactor.

Equating the film growth rate $\alpha E$ with $r_{Si}$, the As incorporation rate from Eqs. (13) and (14) is

$$r_{As}=d_{reg}X_{As}\alpha E+\beta X_{As}^{1/2} . \quad (15)$$

A similar expression holds for P incorporation. The first term is proportional to rf power and is typical of a PECVD growth process. The second term represents a completely different deposition process whose independence of rf power suggests a pyrolytic rather than a plasma-enhanced growth mechanism. This form for $r_{As}$ suggests that two distinct types of As configurations are incorporated into a-Si:H during growth. A regular doping configuration $As^0$ with $r_{As}^0 \propto X_{As}E$ and an irregular nondoping configuration As* with $r_{As}^* \propto X_{As}^{1/2}$. The parameter $\beta$ is the rate constant for irregular impurity incorporation. The data in Fig. 2 give $\beta_{As}/\beta_P \simeq 14$, so that the irregular component of the distribution coefficient, and hence the chemical activity, of arsine is much greater than that of phosphine under low-power growth conditions.

### D. Doping efficiency

According to the chemical equilibrium model presented in Sec. II, the solid-phase As doping efficiency $\eta_{solid} \propto d(As)^{-1}X_{As}^{-1/2}$. When impurity incorporation and, hence, $d$ are regular, the doping efficiency should decrease as the inverse square root of $X$. This is exactly what is observed for both B and P in a-Si:H.[3] However, when impurity incorporation is irregular, deviations from this simple $X^{-1/2}$ dependence should be observed. Indeed, the As doping efficiency ($=[Si_{(3)}^-]/[As]$) shown in Fig. 6 depends strongly on the deposition rate. Under high-power growth conditions, the As distribution coefficient is most nearly regular and the As doping efficiency decreases rapidly with increasing $X_{As}$ as expected. Under low-power growth conditions, the As distribution coefficient is the most irregular and $\eta_{As}$ is essentially constant at between $3\times10^{-3}$ and $5\times10^{-3}$.

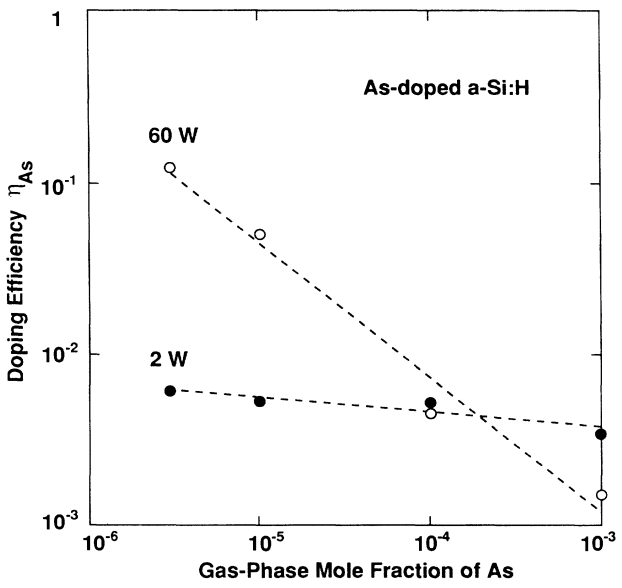


FIG. 6. Solid-phase As doping efficiency as a function of gas-phase As mole fraction for As-doped a-Si:H deposited by rf glow discharge at 2 and 60 W.

Using the analytical expression for $d$(As) [Eq. (13)] derived from fitting to the data, we can understand this behavior more clearly:

$$\eta_{As}\equiv[As_{(4)}^+]/[As] \propto [d(As)]^{-1}X_{As}^{-1/2}$$
$$\propto (d_{reg}X_{As}^{1/2}+\beta/\alpha E)^{-1} . \quad (16)$$

Thus, when incorporation is regular (i.e., $\alpha E$ large and/or $\beta$ small), $\eta_{As} \propto X_{As}^{-1/2}$. On the other hand, when incorporation is irregular (i.e., $\alpha E$ small and/or $\beta$ large), $\eta_{As} \propto \alpha E/\beta \ll 1$. This agrees well with the data in Fig. 6 and clearly shows that the doping efficiency is strongly dependent on both the particular dopant (via $\beta$) and the conditions of dopant incorporation (via $E$).

## IV. DISCUSSION

In summary, we find that (1) a chemical equilibrium model provides a good description of impurity incorporation in a-Si:H, (2) of the three incorporation reactions (6)–(8), only the incorporation of nondoping impurities is irregular, and (3) more excess inactive As than P can be incorporated in the low-power growth limit by a mechanism with the properties given by Eq. (15). We have so far presented an empirical basis for describing impurity incorporation and doping efficiency in a-Si:H. We now consider the growth mechanisms that might lead to the particular form for $d$(As) given in Eq. (13) and their implications.

### A. Two types of As configurations in a-Si:H

Any model of impurity incorporation must explain why the concentration of *active* dopants is not affected by the large enhancement in *total* impurity incorporation in a-Si:H. The problem can be addressed by assuming two types of As configurations in a-Si:H corresponding to two separate modes of impurity incorporation. In other words, only some of the threefold-coordinated As can convert to fourfold-coordinated dopants, but the majority cannot, corresponding to regularly and irregularly incorporated As, respectively. We propose an explanation based on the configuration energy diagram in Fig. 7. This has an $As_{(4)}^+$ level at some energy and an $As_{(3)}^0$ level at a slightly lower energy separated by a small energy barrier. These levels account for the bulk equilibration between doping and nondoping substitutional As configurations and the observation that a nonequilibrium carrier concentration can be "frozen in" by rapid thermal quenching.[11] An identical set of $P_{(3)}^0$ and $P_{(4)}^+$ levels is required to account for the nearly identical defect and carrier concentrations in P-doped a-Si:H.

The diagram has an additional set of configurations, denoted by As* or P* in Fig. 7, which we associate with irregular impurity incorporation. These configurations are highly stable, electronically inactive, and separated by such a large energy barrier from the interconverting two-level configurations that they do not participate in

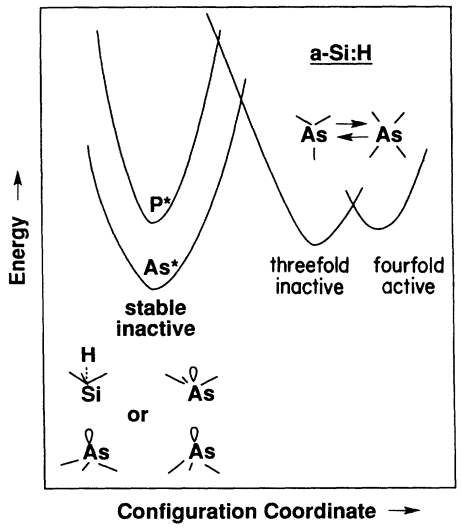


FIG. 7. Configuration energy diagram for P and As impurity incorporation in *a*-Si:H consisting of two sets of metastable threefold- and fourfold-coordinated configurations closely spaced in energy and one stable, electronically inactive set of configurations, possibly consisting of highly relaxed impurity pairs as illustrated in the inset.

the bulk equilibration of the material. The energy of the P* set of configurations is above the $P^{+}_{(4)}$ and $P^{0}_{(3)}$ levels, providing minimal enhancement in the P concentration, while the As* energy levels are below those of the $As^{+}_{(4)}$ and $As^{0}_{(3)}$ configurations, providing for the large enhancements.

The As* configurations are presumably inactive because the bonding geometry is different from normal, isolated $As^{0}_{(3)}$. We suggest two possible types of As* configuration. One possibility is a configuration similar to the $H_2^*$ complex described by Chang and Chadi where either one or both of the Si—H units of the complex is replaced by an As atom.[12] The amorphous network should permit the As atom(s) to more closely attain their desired $p^3$ bonding configuration which should be extremely stable, and the stability of such a configuration should increase with the size of the impurity. This may account for the greater enhancement of As as compared to P incorporation in *a*-Si:H, and predicts an even larger incorporation enhancement of Sb in *a*-Si:H. A second possibility is an isolated As-$H_n$ complex. When As is incorporated with one or more hydrogen bonds, the conversion from threefold to fourfold coordination might be prevented by an increased barrier, or the fourfold-coordinated state might not be a shallow donor.

### B. Two modes of As incorporation in *a*-Si:H

Consider the PECVD incorporation of Si and As as described stoichiometrically by the following surface reactions:[13]

$$Si_{(3)}+SiH_3 \rightarrow SiSiH+H_2 , \tag{17}$$

$$Si_{(3)}+AsH_2 \rightarrow SiAs+H_2 , \tag{18}$$

where $Si_{(3)}$ are surface dangling bonds that act as surface adsorption sites. Neglecting the reverse reactions, the rates of Si and As incorporation are

$$r_{Si}=[Si_{(3)}][SiH_3]k_{Si} , \tag{19}$$

$$r_{As}=[Si_{(3)}][AsH_2]k_{As} . \tag{20}$$

The regular As distribution coefficient is

$$d_{reg}=r_{As}/r_{Si}X_{As}=[AsH_2]k_{As}/[SiH_3]k_{Si}X_{As} =\sigma_{As}k_{As}/\sigma_{Si}k_{Si} , \tag{21}$$

where $\sigma_{As}$ and $\sigma_{Si}$ are the arsine and silane dissociation probabilities, respectively. Thus the regular component of the distribution coefficient is simply the ratio of the efficiencies of As and Si PECVD incorporation, as might be expected.

Because the irregular As incorporation rate is independent of rf plasma power, we conclude the irregular arsenic incorporation must occur through chemical reactions that involve $AsH_3$ molecules rather than $AsH_3$ radicals (i.e., $AsH_2$) or excited states. $AsH_3$ pyrolysis can be described by the following reaction:

$$Si_{(3)}+AsH_3 \leftrightarrows SiAsH_n+Z , \tag{22}$$

where $Z$ is some undetermined species. The concentration of $Z$, or the concentration of any other product in a similar $AsH_3$ pyrolysis reaction, must be proportional to $X_{As}^{1/2}$ in order to account for the $X_{As}^{1/2}$ dependence of the irregular term in the As incorporation rate of Eq. (15). We propose two possibilities, neither completely satisfactory.

If the rate-limiting step of irregular impurity incorporation is the surface attachment and ionization of $AsH_3$, then applying the law of mass action to the reaction

$$Si_{(3)}+AsH_3 \leftrightarrows Si_{(3)}-AsH_3^{+}+e^{-} \tag{23}$$

might give the observed square-root dependence of [As*] on $X_{As}$:

$$r^*_{As} \propto [As^*] \approx [Si_{(3)}-AsH_3^{+}] \propto X_{As}/[e^{-}] \propto X_{As}^{1/2} , \tag{24}$$

when $[e^{-}] \propto X_{As}^{1/2}$ as is observed experimentally.[7] Equation (24) confirms that $d$(As) depends on Fermi level and suggests that even larger values of $d$(As) should be observed in *a*-Si:H counterdoped with B. However, $d$(As) *decreases* when counterdoped with B as shown in Fig. 8. It is also difficult to reconcile the initial ionization step in the above reaction with the observed neutral and very stable final As* configuration.

Alternatively, the rate-limiting step for irregular impurity incorporation might be the thermal dissociation of $AsH_3$ as follows:

$$Si_{(3)}+AsH_3 \leftrightarrows SiAsH+H_2 , \tag{25}$$

where

$$r^*_{As} \propto [SiAsH] \propto [AsH_3]/[H_2] . \tag{26}$$

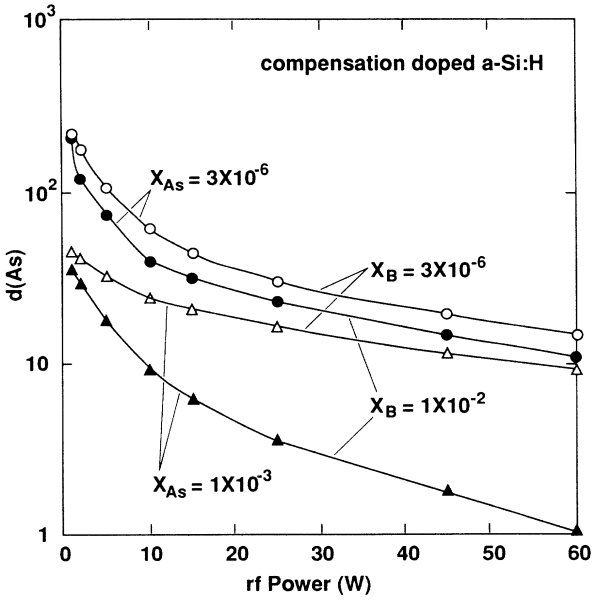


FIG. 8. Distribution coefficient as a function of rf power for As-doped a-Si:H deposited by rf glow discharge with B counterdoping.

It is clear from Eqs. (17) and (25) that the total concentration of $H_2$ in the gas derives from at least two distinct sources: a plasma-enhanced source [Eqs. (17) and (18)] with $[H_2] \propto E$ and a thermal source [Eq. (25)] with $[H_2] \propto [AsH_3]^{1/2}$. In the limit that $E \rightarrow 0$, the thermal source dominates, and $r^*_{As} \propto [AsH_3]^{1/2}$.[14] However, it is difficult to imagine that the thermal generation of $H_2$ could ever be dominant except for growth under conditions where the deposition rates would be negligibly low. In addition, under conditions of high hydrogen dilution, where the largest irregularities are observed, it is very unlikely that the small contribution from $AsH_3$ pyrolysis could significantly affect $H_2$ production.

### C. Effects of other deposition conditions on d(As)

The regular component of the distribution coefficient should be independent of growth temperature $T_s$, gas flow rate $F$, or other deposition parameters. The weak dependence of $d$(As) on flow rate (Fig. 4) and growth temperature (Fig. 5) occurs in a growth regime where irregular As incorporation dominates. Thus it is the irregular component of $d$(As) $[=d_{reg}+d_{irreg}(E,X)]$ that is sensitive to changes in $F$ and $T_s$. An understanding of these effects would provide greater insight into the process of irregular impurity incorporation. We speculate as to the origin of this behavior as follows: Although explicitly included in reactions (23) and (25), we might imagine that $AsH_3$ pyrolysis does not depend on the surface dangling bond concentration $[Si_{(3)}]$. In this case, $d_{irreg}$ would depend inversely on $[Si_{(3)}]$. Increases in the gas flow rate would tend to increase the H overpressure and decrease $[Si_{(3)}]$, while increases in the surface temperature would tend to increase $[Si_{(3)}]$ through increased desorption of H from the surface. Such changes in $[Si_{(3)}]$ could lead to the small variations observed in $d$(As).

On the other hand, it is the regular component of $d$(As) that is most sensitive to counterdoping with B (Fig. 8). Counterdoping decreases $d_{reg}$ by nearly a factor of 10. Because the film deposition rate $r_{Si}$ is not affected, it must be the As PECVD reaction constant alone that is reduced. One possibility to account for this would be a gas-phase reaction between B and As hydrides before actually depositing on the a-Si:H growth surface. In this case, reaction (18) would no longer apply, and one might expect that the incorporation probability for large As-B complexes would be smaller than the corresponding probability of regular As incorporation. More detailed measurements are needed to reduce the speculative nature of the above arguments.

## V. SUMMARY

We have described a chemical equilibrium model of impurity incorporation in a-Si:H and have verified its general applicability by measuring the behavior of As and P incorporation and activation over a wide range of deposition conditions. We find that the impurity incorporation rate can be described by two components: a regular, electronically active PECVD component that depends on plasma power and gas-phase impurity mole fraction $X$ and an irregular, electronically inactive pyrolytic component proportional to the square root of $X$. We have derived an analytical form for the impurity incorporation rate by fitting to the experimental data and have used the result to interpret the measured As doping efficiencies. We have discussed the origin of the $X^{1/2}$ dependence of the irregular impurity incorporation rate, but more work is required before this behavior is fully understood.

## ACKNOWLEDGMENTS

We thank M. Stutzmann for many stimulating discussions. This work supported by the Solar Energy Research Institute (Golden, CO).

*Present address: NTT Basic Research Laboratories, Nippon Telegraph and Telephone Corporation, 3-9-11 Midori-cho, Musashino-shi, Tokyo 180, Japan.

[1]W. E. Spear and P. G. LeComber, Solid State Commun. **17**, 1193 (1975).

[2]J. C. Knights, T. M. Hayes, and J. C. Mikkelsen, Jr., Phys. Rev. Lett. **39**, 712 (1977).

[3]M. Stutzmann, D. K. Biegelsen, and R. A. Street, Phys. Rev. B **35**, 5666 (1987).

[4]K. Winer and R. A. Street, Phys. Rev. Lett. **63**, 880 (1989).

[5]C. C. Tsai, J. C. Knights, G. Chang, and B. Wacker, J. Appl. Phys. **59**, 2998 (1986).

[6]K. Winer and W. B. Jackson, Phys. Rev. B **40**, 12 558 (1989).

[7]R. A. Street, Phys. Rev. Lett. **49**, 1187 (1982); J. Non-Cryst.

Solids **77&78**, 1 (1985); R. A. Street, M. Hack, and W. B. Jackson, Phys. Rev. B **37**, 4209 (1988).
[8]W. B. Jackson and N. M. Amer, Phys. Rev. B **25**, 5559 (1982).
[9]Secondary-ion mass spectroscopy (SIMS) measurements performed with the aid of C. Jones, C. Kirshbaum, and S. Novak at Charles Evans and Associates, Redwood City, CA.
[10]N. M. Johnson, J. Walker, C. M. Doland, K. Winer, and R. A. Street, Appl. Phys. Lett. **54**, 1872 (1989).
[11]R. A. Street, J. Kakalios, and T. M. Hayes, Phys. Rev. B **34**, 3030 (1986).
[12]K. J. Chang and D. J. Chadi, Phys. Rev. Lett. **60**, 2187 (1988).
[13]R. Robertson, D. Hills, H. Chatham, and A. Gallagher, Appl. Phys. Lett. **43**, 544 (1983).
[14]M. Stutzmann (private communication).